

Thick-restarted joint Lanczos bidiagonalization for the GSVD*

Fernando Alvarruiz[†] Carmen Campos[‡] Jose E. Roman[§]

May 15, 2023

Abstract

The computation of the partial generalized singular value decomposition (GSVD) of large-scale matrix pairs can be approached by means of iterative methods based on expanding subspaces, particularly Krylov subspaces. We consider the joint Lanczos bidiagonalization method, and analyze the feasibility of adapting the thick restart technique that is being used successfully in the context of other linear algebra problems. Numerical experiments illustrate the effectiveness of the proposed method. We also compare the new method with an alternative solution via equivalent eigenvalue problems, considering accuracy as well as computational performance. The analysis is done using a parallel implementation in the SLEPc library.

1 Introduction

The generalized singular value decomposition (GSVD) of two matrices was introduced by Van Loan [28], with subsequent additional developments by Paige and Saunders [23]. Given two real matrices A and B with the same number of columns, the GSVD of the pair $\{A, B\}$ is given by

$$U_A^T A G = C, \quad U_B^T B G = S, \quad (1)$$

where U_A, U_B are orthogonal matrices, G is a square nonsingular matrix, and C, S are diagonal matrices in the simplest case. A more precise definition of the problem will be given in section 2.1. This factorization, as an extension of the usual singular value decomposition (SVD), is finding its way in an increasing number of applications, for instance in the solution of constrained least squares problems [12], discrete ill-posed problems via Tikhonov regularization [22, 20], as well as in many other contexts [9].

The problem of computing the GSVD of a small dense matrix pair is well understood, and a robust implementation is available in LAPACK [1, §2.3.5.3]. However, the case of large sparse matrix pairs is still the subject of active research. Normally, the computation of the large-scale GSVD is addressed by means of iterative methods based on expanding subspaces. This is the case of the Jacobi–Davidson method proposed by Hochstenbach [16]. In this paper, we focus on Krylov methods, which still need to incorporate a great deal of the knowledge and innovation that has been successfully applied in similar linear algebra problems such as the SVD. One example of such is an effective restart mechanism, which is the main focus of this paper. The

*This work was supported by the Spanish Agencia Estatal de Investigación under grant PID2019-107379RB-I00 / AEI / 10.13039/501100011033.

[†]D. Sistemes Informàtics i Computació, Universitat Politècnica de València, València, Spain (fbermejo@dsic.upv.es).

[‡]D. Didáctica de la Matemàtica, Universitat de València, València, Spain (carmen.campos-gonzalez@uv.es).

[§]D. Sistemes Informàtics i Computació, Universitat Politècnica de València, València, Spain (jroman@dsic.upv.es).

ultimate goal is to provide reliable software implementations of the methods that are readily available to users from the field of scientific computing or any other discipline that requires computing a GSVD. In our case, the developments presented in this paper are included in one of the solvers of SLEPc, the Scalable Library for Eigenvalue Problem Computations [14].

Zha [30] was the first to propose a Lanczos method to be used for the GSVD. His method relies on a joint bidiagonalization of the two matrices, A and B , in a similar way as Lanczos methods for the SVD have a single bidiagonalization in their foundation. The joint bidiagonalization in Zha's method results in two small-sized upper bidiagonal matrices. Later, Kilmer and coauthors [22] proposed a variant in which one of the two bidiagonal matrices generated by the joint bidiagonalization is lower instead of upper. The latter has since then been the most popular approach, and we focus mainly on that variant for our developments.

As in any Lanczos method, a finite-precision arithmetic implementation suffers from various numerical pitfalls, such as loss of orthogonality in the generated Krylov basis vectors. Jia and Li [19] have studied numerical error in the context of joint bidiagonalization for the GSVD, showing that loss of orthogonality can be prevented by simply enforcing semiorthogonality of Lanczos vectors, e.g., with a partial reorthogonalization technique [18], as is done in Lanczos methods for other linear algebra problems. Either in the case that a semiorthogonality scheme is pursued, or a full reorthogonalization approach is followed as we do to avoid loss of orthogonality, a consequence is that all Lanczos vectors must be kept throughout the computation, with the consequent increase in storage and computational costs.

Thick restart is an effective mechanism to keep the size of the Krylov basis bounded, that has been applied to Lanczos methods in many different contexts such as the symmetric eigenproblem [29] or the SVD [2, 15]. Compared to explicit restart, the thick restart scheme is much more effective because it compresses the currently available Krylov subspace into another Krylov subspace of smaller dimension (not a single vector), that retains the wanted spectral information while purging the components associated with unwanted eigenvalues (or singular values). The thick restart methodology can be summarized in two stages. In the first stage, one or more Lanczos recurrences are used to build one or more sets of Lanczos vectors, in a way that the small-sized problem resulting from the projection of the original problem retains the properties of the original problem (structure preservation). For instance, for symmetric-indefinite matrix pencils it is possible to employ a pseudo-Lanczos recurrence that results in a symmetric-indefinite projected problem [5]. In the second stage, the built factorization is truncated to a smaller size decomposition, in a way that it is feasible to extend it again using the same Lanczos recurrences.

In this paper, we work out the details that are needed for thick-restarting the Lanczos recurrences associated with the joint bidiagonalization for the GSVD, so that the projected problem is a small-size GSVD, and this structure is preserved whenever the restart truncates the involved decompositions and they are extended again.

The rest of the paper is organized as follows. Section 2 presents all the background material that is required for section 3, which presents the new developments related to thick restart for the GSVD. In section 4 we provide a few details of how the proposed method has been implemented in the SLEPc library. Section 5 illustrates how the solver performs when applied to several test problems. Finally, we wrap up with some concluding remarks in section 6. Throughout the paper, the presentation is done for real matrices, although the extension to the complex case is straightforward. In fact, our implemented solver supports both real and complex arithmetic.

2 Background

In this section, we review a number of concepts that are required for the developments of subsequent sections. Many of the concepts are also discussed for the case of the SVD, aiming

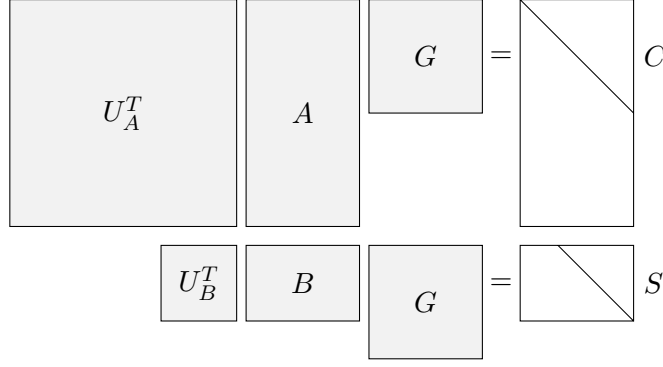


Figure 1: Scheme of the GSVD of two matrices A and B , for the case $m > n$ and $p < n$.

$s_{q+1} \leq \dots \leq s_{q+\ell}$, we have that $c_i^2 + s_i^2 = 1$, $i = q + 1, \dots, q + \ell$, and the generalized singular values $\sigma(A, B)$ are the ratios of these quantities,

$$\underbrace{\infty, \dots, \infty}_q, \underbrace{c_{q+1}/s_{q+1}, \dots, c_{q+\ell}/s_{q+\ell}}_\ell, \underbrace{0, \dots, 0}_{n-q-\ell}. \quad (7)$$

In order to better understand the structure of C and S , it is helpful to note that the zero blocks in (6) may have zero rows or columns, and also that the number of nonzero rows of C is equal to $\text{rank}(A)$ and similarly for S with respect to $\text{rank}(B)$. For instance, fig. 1 shows an example of GSVD for the case that $m > n$ and $p < n$. Assuming that A and B have full column and row ranks, respectively, we have that there are $q = n - p$ infinite generalized singular values.

As in the case of the SVD, for large-scale problems we will consider a partial GSVD, that is, we employ methods that compute approximations of k quadruples $(\sigma_i, u_i^A, u_i^B, g_i)$ corresponding to either the largest or the smallest generalized singular values σ_i . We call u_i^A and u_i^B the left generalized singular vectors, while g_i are the right generalized singular vectors. Note that if σ_i are the generalized singular values of $\{A, B\}$, then σ_i^{-1} are the generalized singular values of $\{B, A\}$.

2.2 Equivalent eigenvalue problems

The solution of the two problems presented in the previous section can be approached by formulating a related eigenvalue problem. More precisely, there are two possible strategies, that we will refer to as *cross* and *cyclic*. We start by discussing this in the context of the SVD and then extend it to the GSVD.

The SVD relation (2) can be written as $AV = U\Sigma$ or as $A^T U = V\Sigma^T$. Suppose that $m \geq n$, then equating the columns we have

$$Av_i = u_i \sigma_i, \quad i = 1, \dots, n, \quad (8)$$

$$A^T u_i = v_i \sigma_i, \quad i = 1, \dots, n, \quad (9)$$

$$A^T u_i = 0, \quad i = n + 1, \dots, m. \quad (10)$$

Premultiplying (8) by A^T and using (9) results in the relation

$$A^T Av_i = \sigma_i^2 v_i, \quad (11)$$

that is, the v_i are the eigenvectors of the symmetric matrix $A^T A$ corresponding to eigenvalues σ_i^2 . If the corresponding left singular vectors are also required, they can be computed as $u_i = \frac{1}{\sigma_i} Av_i$

from (8). Alternatively, it is possible to compute the left vectors first, via

$$AA^T u_i = \sigma_i^2 u_i, \quad (12)$$

and then the right ones as $v_i = \frac{1}{\sigma_i} A^T u_i$, but care must be taken that (12) has at least $m - n$ zero eigenvalues. In practice, one would generally use (11) if $m \geq n$ and (12) otherwise. We will call this approach the cross product eigenproblem.

The second strategy is the cyclic eigenproblem. Consider the symmetric matrix of order $m + n$

$$H(A) = \begin{bmatrix} 0 & A \\ A^T & 0 \end{bmatrix}, \quad (13)$$

that has eigenvalues $\pm\sigma_i$, $i = 1, \dots, r$, together with $m + n - 2r$ zero eigenvalues, where $r = \text{rank}(A)$. The normalized eigenvectors corresponding to $\pm\sigma_i$ are $\frac{1}{\sqrt{2}} \begin{bmatrix} \pm u_i \\ v_i \end{bmatrix}$. Hence we can extract the singular triplets (σ_i, u_i, v_i) of A directly from the eigenpairs of $H(A)$. Note that in this case the singular values are not squared, so the computed smallest singular values will not suffer from severe loss of accuracy as in the cross product approach. The drawback in this case is that small eigenvalues are located in the interior of the spectrum.

The cross and cyclic schemes can also be applied to the GSVD (1). The columns of G satisfy

$$s_i^2 A^T A g_i = c_i^2 B^T B g_i, \quad (14)$$

so solving a symmetric-definite generalized eigenvalue problem for the pencil $(A^T A, B^T B)$ provides us with the generalized singular values and right generalized singular vectors. From g_i we can compute $u_i^A = \frac{1}{c_i} A g_i$ and $u_i^B = \frac{1}{s_i} B g_i$. This is the analog of the cross product eigenproblem for the SVD (11). It has the same concerns regarding the loss of accuracy in the smallest generalized singular values, but in this case one may consider computing these values as the reciprocals of the largest eigenvalues of the reversed pencil $(B^T B, A^T A)$.

Likewise, the formulation that is analogous to the eigenproblem associated with the cyclic matrix (13) is to solve the symmetric-definite generalized eigenvalue problem defined by any of the matrix pencils

$$\left(\begin{bmatrix} 0 & A \\ A^T & 0 \end{bmatrix}, \begin{bmatrix} I & 0 \\ 0 & B^T B \end{bmatrix} \right), \quad \text{or} \quad \left(\begin{bmatrix} 0 & B \\ B^T & 0 \end{bmatrix}, \begin{bmatrix} I & 0 \\ 0 & A^T A \end{bmatrix} \right), \quad (15)$$

of dimensions $m + n$ and $p + n$, respectively. The nonzero eigenvalues of the first pencil are $\pm\sigma_i$, while those of the second pencil are $\pm\sigma_i^{-1}$, so the latter is likely to be preferred when the smallest generalized singular values are required. The generalized singular vectors can be obtained from the eigenvectors corresponding to nonzero eigenvalues $\pm\sigma_i$ of the first pencil, $\frac{1}{\sqrt{2}} \begin{bmatrix} u_i^A \\ \pm g_i/s_i \end{bmatrix}$, or the second pencil, $\frac{1}{\sqrt{2}} \begin{bmatrix} u_i^B \\ \pm g_i/c_i \end{bmatrix}$. See [17] for considerations on which of the two pencils is best in finite precision computations, based on the conditioning of A and B .

Note that the symmetric-definite generalized eigenproblems discussed in this section may in fact be semi-definite, e.g., if $B^T B$ is singular because $p < n$. This may cause numerical difficulties when solving the problem via the cross and cyclic approaches.

2.3 SVD via Lanczos bidiagonalization

In this section we give an overview of the computation of the partial SVD by means of Lanczos recurrences. Additional details can be found, e.g., in [15]. Without loss of generality, we will assume that A is tall, i.e., $m \geq n$.

In the same way that the solution of the cross product eigenproblem for $A^T A$ can be approached by first computing an orthogonal similarity transformation to tridiagonal form, bidiagonalization methods for the SVD rely on an orthogonal reduction to bidiagonal form,

$$A = P_n J_n Q_n^T, \quad (16)$$

with $P_n \in \mathbb{R}^{m \times n}$ and $Q_n \in \mathbb{R}^{n \times n}$ having orthonormal columns and $J_n \in \mathbb{R}^{n \times n}$ being upper bidiagonal, so that $J_n^T J_n$ is tridiagonal with eigenvalues σ_i^2 , that is, J_n has the same singular values as A .

In a Lanczos method, we compute a partial bidiagonalization instead of the full one. From (16) we can establish the two equalities $AQ_n = P_n J_n$ and $A^T P_n = Q_n J_n^T$, and equating the first $k < n$ columns we obtain the Lanczos relations

$$AQ_k = P_k J_k, \quad (17)$$

$$A^T P_k = Q_k J_k^T + \beta_k q_{k+1} e_k^T, \quad (18)$$

where J_k denotes the $k \times k$ leading principal submatrix of J_n , and we have used the notation

$$J_k = \begin{bmatrix} \alpha_1 & \beta_1 & & & & \\ & \alpha_2 & \beta_2 & & & \\ & & \ddots & \ddots & & \\ & & & \alpha_{k-1} & \beta_{k-1} & \\ & & & & & \alpha_k \end{bmatrix}. \quad (19)$$

Equating the j th column of (17)-(18) gives the familiar double Lanczos recurrence that is shown in algorithmic form in algorithm 1.

ALGORITHM 1: Lanczos bidiagonalization

Input: Matrix $A \in \mathbb{R}^{m \times n}$, unit-norm vector $q_1 \in \mathbb{R}^n$, number of steps k .

Output: Partial bidiagonalization (17)-(18).

- 1: Set $\beta_0 = 0$
 - 2: **for** $j = 1, 2, \dots, k$ **do**
 - 3: $p_j = Aq_j - \beta_{j-1}p_{j-1}$
 - 4: Normalize: $\alpha_j = \|p_j\|_2$, $p_j = p_j/\alpha_j$
 - 5: $q_{j+1} = A^T p_j - \alpha_j q_j$
 - 6: Normalize: $\beta_j = \|q_{j+1}\|_2$, $q_{j+1} = q_{j+1}/\beta_j$
 - 7: **end for**
-

It is possible to establish an equivalence between the output of algorithm 1 and the quantities computed by the Lanczos recurrence for tridiagonalizing the cross product matrix $A^T A$, see for instance [15]. In particular, the right Lanczos vectors q_j computed by algorithm 1 form an orthonormal basis of the Krylov subspace $\mathcal{K}_k(A^T A, q_1)$. Similarly, the left Lanczos vectors p_j span the Krylov subspace $\mathcal{K}_k(AA^T, Aq_1)$. Finally, there is also an equivalence with the Lanczos tridiagonalization associated with the cyclic matrix (13), provided that the initial vector $[0^T q_1^T]^T$ is used.

From the discussion above, it is clear that Ritz approximations of the singular triplets of A can be obtained. After k Lanczos steps, the Ritz values $\tilde{\sigma}_i$ (approximate singular values of A) are computed as the singular values of J_k , and the Ritz vectors are $\tilde{u}_i = P_k x_i$ and $\tilde{v}_i = Q_k y_i$, where x_i and y_i are the left and right singular vectors of J_k , respectively.

2.4 Residual and stopping criterion

As the number of Lanczos steps increase, the Ritz approximations become increasingly accurate. A criterion is required to determine when a certain approximate singular triplet $(\tilde{\sigma}_i, \tilde{u}_i, \tilde{v}_i)$ can be declared converged. And for this, we need to define a residual.

Due to the equivalence discussed in section 2.2, we can define the residual in terms of an equivalent eigenproblem. In the case of the cross product eigenproblem, (11) or (12), only one of the singular vectors would appear, so it is better to define the residual vector in terms of the eigenproblem associated with the cyclic matrix (13), whose norm is

$$\|r_i^{\text{SVD}}\|_2 = \sqrt{\|A\tilde{v}_i - \tilde{\sigma}_i\tilde{u}_i\|_2^2 + \|A^T\tilde{u}_i - \tilde{\sigma}_i\tilde{v}_i\|_2^2}. \quad (20)$$

This residual norm can be used in a posteriori error bounds. In particular, there exists a singular value $\sigma_{i'}$ of A such that $|\sigma_{i'} - \tilde{\sigma}_i| \leq \frac{1}{\sqrt{2}}\|r_i^{\text{SVD}}\|_2$ [3].

In the context of Lanczos, the residual (20) can be computed cheaply as follows. If the Lanczos relations (17) and (18) are multiplied on the right respectively by y_i and x_i , the right and left singular vectors of J_k , then

$$A\tilde{v}_i = \tilde{\sigma}_i\tilde{u}_i, \quad A^T\tilde{u}_i = \tilde{\sigma}_i\tilde{v}_i + \beta_k q_{k+1} e_k^T x_i,$$

and therefore

$$\|r_i^{\text{SVD}}\|_2 = \beta_k |e_k^T x_i|. \quad (21)$$

The residual estimate (21) can be used in the stopping criterion in practical implementations of Lanczos bidiagonalization.

2.5 Thick restart for the SVD

As in any Lanczos process, when run in finite precision arithmetic, loss of orthogonality among Lanczos vectors occurs in algorithm 1 whenever the Ritz values start to converge. The simplest cure is full reorthogonalization, which we consider in this work. This solution would be implemented by replacing line 3 of algorithm 1 with

$$p_j = \text{orthog}(Aq_j, P_{j-1})$$

that applies Gram-Schmidt to explicitly orthogonalize vector Aq_j against the columns of P_{j-1} , and similarly for line 5.

Full reorthogonalization requires keeping all previously computed (left and right) Lanczos vectors, and this justifies the need of a restart technique that limits the number of vectors, not only due to storage requirements but also because the computational cost of full reorthogonalization is proportional to the number of involved vectors.

Thick restart is very effective compared to explicit restart, because instead of explicitly building a new initial vector to rerun the algorithm, it keeps a smaller dimensional subspace that retains the most relevant spectral information computed so far. The computation is thus a sequence of subspace expansions and contractions, until the subspace contains enough converged solutions. The key is to purge unwanted components during the contraction, which is beneficial for overall convergence.

Suppose we have built the Lanczos relations (17)-(18) of order k and we want to compress to size $r < k$. We start by transforming the decomposition in a way that approximate singular values and the residual norms (21) appear explicitly in the equations, as follows. First, compute the

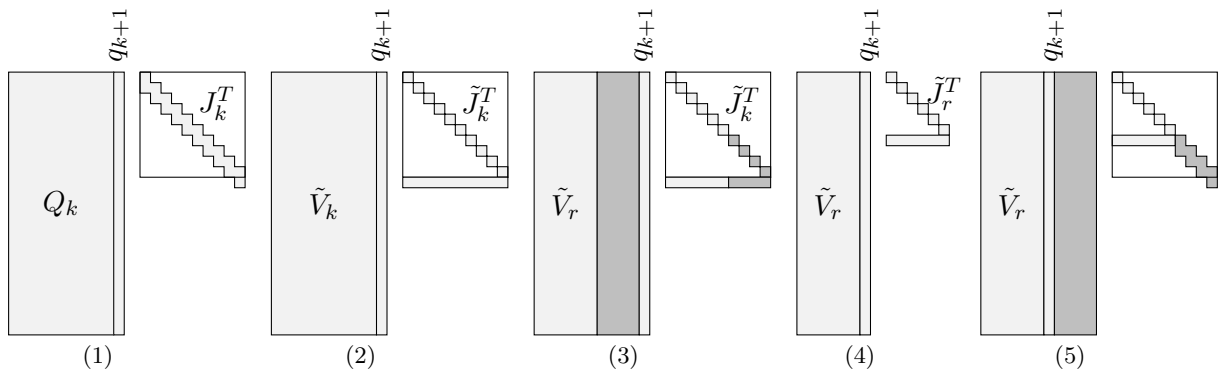


Figure 2: Illustration of the five steps of thick restart in SVD: (1) initial Lanczos factorization of order k , (2) solve projected problem, (3) sort and check convergence, (4) truncate to factorization of order r , and (5) extend to a factorization of order k .

SVD of the bidiagonal matrix, $J_k = X_k \tilde{\Sigma}_k Y_k^T$, with $\tilde{\Sigma}_k = \text{diag}(\tilde{\sigma}_1, \dots, \tilde{\sigma}_k)$. Post-multiplication of (17)-(18) by Y_k and X_k , respectively, results in

$$A \tilde{V}_k = \tilde{U}_k \tilde{\Sigma}_k, \quad (22)$$

$$A^T \tilde{U}_k = \tilde{V}_k \tilde{\Sigma}_k + \beta_k q_{k+1} e_k^T X_k, \quad (23)$$

where $\tilde{U}_k = P_k X_k$ and $\tilde{V}_k = Q_k Y_k$, whose columns are the left and right Ritz vectors. This would be an exact partial SVD of A if it were not for the second summand of the right-hand side of (23), which is related to the residual norms of the k Ritz approximations. Equation (23) can also be written as

$$A^T \tilde{U}_k = [\tilde{V}_k \quad q_{k+1}] \tilde{J}_k^T, \quad \tilde{J}_k = \begin{bmatrix} \tilde{\sigma}_1 & & \rho_1 \\ & \tilde{\sigma}_2 & \rho_2 \\ & & \ddots & \vdots \\ & & & \tilde{\sigma}_k & \rho_k \end{bmatrix}, \quad (24)$$

where $\rho_i := \beta_k e_k^T x_i$. Note that $|\rho_i|$ is equal to the residual norm (21). Equation (24) is represented graphically in fig. 2 (step 2).

Due to the fact that $\tilde{\Sigma}_k$ in (22)-(23) is diagonal, it is possible to truncate this decomposition at any size r . For this, we must permute it so that the leading principal submatrix of $\tilde{\Sigma}_k$ contains the approximations of the wanted singular values (typically the largest or smallest ones). Figure 2 (step 3) shows in dark gray the part of the decomposition that will be discarded. Then the new decomposition after truncation is

$$A \tilde{V}_r = \tilde{U}_r \tilde{\Sigma}_r,$$

$$A^T \tilde{U}_r = \tilde{V}_r \tilde{\Sigma}_r + q_{k+1} b_r^T,$$

where $b_r^T = [\rho_1, \dots, \rho_r]$, see fig. 2 (step 4). It only remains to extend the decomposition by running a modified version of algorithm 1 that starts the loop at $j = r + 1$. Note that the first newly generated left Lanczos vector is computed as $p_{r+1} = \text{orthog}(A q_{k+1}, \tilde{U}_r)$, whose orthogonalization coefficients are precisely the ρ_i 's. When the algorithm stops at iteration $j = k$, the new J_k matrix has the shape depicted in fig. 2 (step 5), a bidiagonal except for the leading part that has an arrowhead form.

2.6 GSVD via joint Lanczos bidiagonalization

We now turn our attention to the GSVD, and consider Lanczos methods that compute a joint bidiagonalization of the two matrices, A and B . In this context, the stacked matrix Z (5) is relevant and will appear in the algorithms. Also, the matrices Q_A and Q_B in (5), whose row dimensions are the same as A and B , respectively, will be used for deriving the methods, but need not be formed explicitly as justified later.

The matrices C and S (6) are related to the CS decomposition [12, §2.6.4] of $\{Q_A, Q_B\}$, that is, the values c_i and s_i are related to the singular values of Q_A and Q_B , respectively. Let the CS decomposition of $\{Q_A, Q_B\}$ be

$$Q_A = U_A C W^T, \quad Q_B = U_B S W^T, \quad (25)$$

where U_A, U_B are the same as in (4), and $W \in \mathbb{R}^{n \times n}$ is also orthogonal. Note that the first equation in (25) can be seen as the conventional SVD of Q_A , with the singular values sorted in non-increasing order, while the second equation is an SVD-like relation where the singular values appear in non-decreasing order with the largest value at the bottom-right corner of S .

If Z has full column rank, the GSVD decomposition of $\{A, B\}$ is given by

$$A = U_A C G^{-1}, \quad B = U_B S G^{-1}, \quad (26)$$

where $G = R^{-1}W$ with R as defined in (5).

An approach to compute the CS decomposition of $\{Q_A, Q_B\}$ is to perform a bidiagonalization of both matrices, i.e., a decomposition of the form

$$Q_A = U J V^T, \quad Q_B = \hat{U} \hat{J} V^T, \quad (27)$$

with J, \hat{J} (upper or lower) bidiagonal matrices such that the stacked matrix $\begin{bmatrix} J \\ \hat{J} \end{bmatrix}$ has orthonormal columns, that is, $J^T J + \hat{J}^T \hat{J} = I$. Then, the problem is reduced to the CS decomposition of the bidiagonal matrices $\{J, \hat{J}\}$,

$$J = X C Y^T, \quad \hat{J} = \hat{X} S Y^T. \quad (28)$$

Substituting in (27) we get the CS decomposition (25) with $U_A = U X$, $U_B = \hat{U} \hat{X}$ and $W = V Y$.

As mentioned in section 2.1, if A, B are very large and sparse matrices, the interest is normally to compute a partial decomposition, i.e., a few (extreme) generalized singular values and vectors. In that case, a partial bidiagonalization of matrices Q_A and Q_B is done using Lanczos recurrences, as described next.

Zha [30] presented an algorithm for the joint bidiagonalization of Q_A and Q_B , in which both matrices are reduced to upper bidiagonal form without explicitly computing Q_A or Q_B . Later, Kilmer *et al.* [22] proposed a variation of the joint bidiagonalization where Q_A and Q_B are transformed to lower and upper bidiagonal forms, respectively. To keep the presentation short, we focus on the latter variant from now on, although our solver also includes an implementation of Zha's variant.

Although not computing Q_A or Q_B explicitly, Kilmer's joint bidiagonalization is based on the application of the lower and upper Lanczos bidiagonalization algorithms in [24] to Q_A and Q_B , respectively, yielding

$$Q_A V_k = U_{k+1} J_k, \quad Q_A^T U_{k+1} = V_k J_k^T + \alpha_{k+1} v_{k+1} e_{k+1}^T, \quad (29)$$

$$Q_B \hat{V}_k = \hat{U}_k \hat{J}_k, \quad Q_B^T \hat{U}_k = \hat{V}_k \hat{J}_k^T + \hat{\beta}_k \hat{v}_{k+1} e_k^T, \quad (30)$$

with the column-orthonormal matrices $U_{k+1} = [u_1, u_2, \dots, u_{k+1}]$, $V_k = [v_1, v_2, \dots, v_k]$, $\hat{U}_k = [\hat{u}_1, \hat{u}_2, \dots, \hat{u}_k]$ and $\hat{V}_k = [\hat{v}_1, \hat{v}_2, \dots, \hat{v}_k]$ and the lower and upper bidiagonal matrices

$$J_k = \begin{bmatrix} \alpha_1 & & & & & \\ \beta_2 & \alpha_2 & & & & \\ & \ddots & \ddots & & & \\ & & & \beta_k & \alpha_k & \\ & & & & \beta_{k+1} & \end{bmatrix} \in \mathbb{R}^{(k+1) \times k}, \quad \hat{J}_k = \begin{bmatrix} \hat{\alpha}_1 & \hat{\beta}_1 & & & & \\ & \hat{\alpha}_2 & \ddots & & & \\ & & \ddots & \ddots & & \\ & & & \ddots & \hat{\beta}_{k-1} & \\ & & & & \hat{\alpha}_k & \end{bmatrix} \in \mathbb{R}^{k \times k}.$$

Note that the bottom Lanczos relations (30) are analogous to those used for the bidiagonalization in SVD (17)-(18). However, the top Lanczos relations (29) differ in that the associated bidiagonal matrix J_k is lower bidiagonal with one more row than columns, and the basis of left Lanczos vectors U_{k+1} contains one more vector than in the other case. The reason is that the lower bidiagonalization algorithm in [24] starts the recurrence with the left vectors instead of the right ones.

Zha's method generates two upper bidiagonal matrices by applying algorithm 1 to both Q_A and Q_B with the same initial vector. In contrast, Kilmer's method uses the two types of bidiagonalizations and connects them by using the first right Lanczos vector v_1 generated in (29) as initial vector \hat{v}_1 in (30).

It can be shown [30, 22] that if $v_1 = \hat{v}_1$, the joint bidiagonalization given by (29)-(30) verifies

$$\hat{v}_i = (-1)^{i-1} v_i, \quad \hat{\alpha}_i \hat{\beta}_i = \alpha_{i+1} \beta_{i+1}, \quad i = 1, 2, \dots \quad (31)$$

Thus, (29)-(30) can be rewritten as

$$Q_A V_k = U_{k+1} J_k, \quad Q_A^T U_{k+1} = V_k J_k^T + \alpha_{k+1} v_{k+1} e_{k+1}^T, \quad (32)$$

$$Q_B V_k = \hat{U}_k \check{J}_k, \quad Q_B^T \hat{U}_k = V_k \check{J}_k^T + \check{\beta}_k v_{k+1} e_k^T, \quad (33)$$

where $\check{J}_k = \hat{J}_k D$, $D = \text{diag}(1, -1, \dots, (-1)^{k-1})$ and $\check{\beta}_k = (-1)^k \hat{\beta}_k$.

Taking into account that $Q_A = [I_m \ 0] Q$, $Q_B = [0 \ I_p] Q$, and premultiplying equalities on the right side of (32)-(33) by Q , we get

$$[I_m \ 0] Q V_k = U_{k+1} J_k, \quad Q Q^T \begin{bmatrix} U_{k+1} \\ 0 \end{bmatrix} = Q V_k J_k^T + \alpha_{k+1} Q v_{k+1} e_{k+1}^T,$$

$$[0 \ I_p] Q V_k = \hat{U}_k \check{J}_k, \quad Q Q^T \begin{bmatrix} 0 \\ \hat{U}_k \end{bmatrix} = Q V_k \check{J}_k^T + \check{\beta}_k Q v_{k+1} e_k^T,$$

or, defining $\tilde{V}_k = Q V_k$,

$$[I_m \ 0] \tilde{V}_k = U_{k+1} J_k, \quad Q Q^T \begin{bmatrix} U_{k+1} \\ 0 \end{bmatrix} = \tilde{V}_k J_k^T + \alpha_{k+1} \tilde{v}_{k+1} e_{k+1}^T, \quad (34)$$

$$[0 \ I_p] \tilde{V}_k = \hat{U}_k \check{J}_k, \quad Q Q^T \begin{bmatrix} 0 \\ \hat{U}_k \end{bmatrix} = \tilde{V}_k \check{J}_k^T + \check{\beta}_k \tilde{v}_{k+1} e_k^T. \quad (35)$$

The joint bidiagonalization process in [22] uses the two Lanczos relations in (34) and the first one in (35) to compute matrices U_{k+1} , \hat{U}_k , \tilde{V}_k , J_k , \check{J}_k . Recall that the vectors u_j , \hat{u}_j , \tilde{v}_j have lengths m , p and $m+p$, respectively. Algorithm 2 gives the details of Kilmer's joint bidiagonalization, where in lines 2 and 9 $\text{expand}(A, B, u_{j+1})$ denotes the operation that generates new Krylov directions from the A and B matrices as follows. Each step j of the joint bidiagonalization requires computing $Q Q^T \tilde{u}_{j+1}$, where $\tilde{u}_{j+1} = [u_{j+1}^T, 0]^T$. Note that this is the orthogonal

projection of \tilde{u}_{j+1} onto the column space of Z , which means that $QQ^T\tilde{u}_{j+1} = Zx_{j+1}$, where x_{j+1} is the solution of the least squares problem

$$x_{j+1} = \arg \min_{x \in \mathbb{R}^n} \|Zx - \tilde{u}_{j+1}\|. \quad (36)$$

The $\text{expand}(A, B, u_{j+1})$ operation first computes the solution of the least squares problem (36) by padding u_{j+1} below with p zeros, and then performs an additional multiplication by Z . If Z is a large sparse matrix, the least squares problem is solved by means of an iterative solver such as the LSQR algorithm [24]. Thus, the bidiagonalization process does not need to compute the QR factorization of Z .

ALGORITHM 2: Lower-upper joint Lanczos bidiagonalization [22]

Input: Matrices $A \in \mathbb{R}^{m \times n}$, $B \in \mathbb{R}^{p \times n}$, unit-norm vector $u_1 \in \mathbb{R}^n$, number of steps k .

Output: Partial joint bidiagonalization (34)-(35).

- 1: Set $\hat{\beta}_0 = 0$
 - 2: $\tilde{v}_1 = \text{expand}(A, B, u_1)$
 - 3: Normalize: $\alpha_1 = \|\tilde{v}_1\|_2$, $\tilde{v}_1 = \tilde{v}_1/\alpha_1$
 - 4: **for** $j = 1, 2, \dots, k$ **do**
 - 5: $\hat{u}_j = (-1)^{j-1} [0, I_p] \tilde{v}_j - \hat{\beta}_{j-1} \hat{u}_{j-1}$
 - 6: Normalize: $\hat{\alpha}_j = \|\hat{u}_j\|_2$, $\hat{u}_j = \hat{u}_j/\hat{\alpha}_j$
 - 7: $u_{j+1} = [I_m, 0] \tilde{v}_j - \alpha_j u_j$
 - 8: Normalize: $\beta_{j+1} = \|u_{j+1}\|_2$, $u_{j+1} = u_{j+1}/\beta_{j+1}$
 - 9: $\tilde{v}_{j+1} = \text{expand}(A, B, u_{j+1}) - \beta_{j+1} \tilde{v}_j$
 - 10: Normalize: $\alpha_{j+1} = \|\tilde{v}_{j+1}\|_2$, $\tilde{v}_{j+1} = \tilde{v}_{j+1}/\alpha_{j+1}$
 - 11: $\hat{\beta}_j = (\alpha_{j+1}\beta_{j+1})/\hat{\alpha}_j$
 - 12: **end for**
-

After running algorithm 2 we get matrices $U_{k+1}, \hat{U}_k, \tilde{V}_k, J_k, \check{J}_k$ that, taking $V_k = Q^T \tilde{V}_k$, satisfy equations (32)-(33). On the other hand, as pointed out in [22], it can be shown that $J_k^T J_k + \check{J}_k^T \check{J}_k = I_k$, which means that the matrix pair $\{J_k, \check{J}_k\}$ admits a CS decomposition

$$J_k = X_{k+1} \begin{bmatrix} C_k \\ 0 \end{bmatrix} Y_k^T, \quad \check{J}_k = \hat{X}_k S_k Y_k^T, \quad (37)$$

where $X_{k+1} \in \mathbb{R}^{(k+1) \times (k+1)}$, $\hat{X}_k, Y_k \in \mathbb{R}^{k \times k}$ are orthogonal matrices, and C_k, S_k are $k \times k$ diagonal matrices. Note that these matrices do not correspond to subblocks of the matrices X, \hat{X}, Y, C, S appearing in (28).

Using the CS decomposition (37), the Lanczos relations (32)-(33) become

$$Q_A V_k Y_k = U_{k+1} X_{k+1} \begin{bmatrix} C_k \\ 0 \end{bmatrix}, \quad Q_A^T U_{k+1} X_{k+1} = V_k Y_k \begin{bmatrix} C_k & 0 \end{bmatrix} + \alpha_{k+1} v_{k+1} e_{k+1}^T X_{k+1}, \quad (38)$$

$$Q_B V_k Y_k = \hat{U}_k \hat{X}_k S_k, \quad Q_B^T \hat{U}_k \hat{X}_k = V_k Y_k S_k + \check{\beta}_k v_{k+1} e_k^T \hat{X}_k. \quad (39)$$

Taking $\tilde{w}_i, \tilde{u}_i^A, \tilde{u}_i^B, x_i, \hat{x}_i$ and y_i as the i th columns of $V_k Y_k, U_{k+1} X_{k+1}, \hat{U}_k \hat{X}_k, X_k, \hat{X}_k$ and Y_k , respectively, and \tilde{c}_i, \tilde{s}_i , as the i th diagonal elements of C_k, S_k , we have

$$Q_A \tilde{w}_i = \tilde{c}_i \tilde{u}_i^A, \quad Q_A^T \tilde{u}_i^A = \tilde{c}_i \tilde{w}_i + \alpha_{k+1} v_{k+1} e_{k+1}^T x_i, \quad (40)$$

$$Q_B \tilde{w}_i = \tilde{s}_i \tilde{u}_i^B, \quad Q_B^T \tilde{u}_i^B = \tilde{s}_i \tilde{w}_i + \check{\beta}_k v_{k+1} e_k^T \hat{x}_i, \quad (41)$$

for $i = 1, 2, \dots, k$. Thus, $\tilde{u}_i^A, \tilde{u}_i^B$, are approximations of the left generalized singular vectors for A and B , respectively, while the approximate right singular vectors $\tilde{g}_i = R^{-1} \tilde{w}_i$ can be computed as the solution to the least squares problem $Z \tilde{g}_i = \hat{w}_i$, where $\hat{w}_i = Q \tilde{w}_i = Q V_k y_i = \tilde{V}_k y_i$.

3 Thick restart for the GSVD

With all the ingredients presented in the previous section, we are now able to adapt the thick restart technique of section 2.5 to the case of Kilmer's joint bidiagonalization for the GSVD. As was done for the SVD, the goal is to successively compress and expand the decomposition until the working Lanczos bases contain sufficiently good approximations to the wanted solutions. The compression is carried out by transforming the decomposition computed by algorithm 2 to a form where the generalized singular values (or, more precisely, the c_i and s_i values) appear explicitly, and then truncating it in a way that keeps the most relevant part. This requires computing a small-sized GSVD (or CS decomposition), as in (37). Once the decomposition is truncated, it should be possible to extend it again by a slightly modified variant of algorithm 2 whose loop starts at the current size after truncation.

3.1 Restarting Kilmer's joint bidiagonalization

Substituting (37) in (34)-(35), we have

$$\begin{aligned} [I_m \ 0] \tilde{V}_k Y_k &= U_{k+1} X_{k+1} \begin{bmatrix} C_k \\ 0 \end{bmatrix}, & QQ^T \begin{bmatrix} U_{k+1} X_{k+1} \\ 0 \end{bmatrix} &= \tilde{V}_k Y_k [C_k \ 0] + \alpha_{k+1} \tilde{v}_{k+1} e_{k+1}^T X_{k+1}, \\ [0 \ I_p] \tilde{V}_k Y_k &= \hat{U}_k \hat{X}_k S_k, & QQ^T \begin{bmatrix} 0 \\ \hat{U}_k \hat{X}_k \end{bmatrix} &= \tilde{V}_k Y_k S_k + \check{\beta}_k \tilde{v}_{k+1} e_k^T \hat{X}_k. \end{aligned}$$

This decomposition is similar to (38)-(39), but expressed in terms of the \tilde{V}_k basis instead of V_k .

In order to truncate the equations above, we define Y_r and \hat{X}_r as the matrices formed by taking the first r columns of Y_k and \hat{X}_k , respectively, C_r and S_r as the leading principal $r \times r$ submatrix of C_k and S_k , and $X_{r+1} = [x_1, x_2, \dots, x_r, x_{k+1}]$, where x_j is column j of X_{k+1} . Note that we keep the last column x_{k+1} and append it as column $r+1$. We can then write

$$\begin{aligned} [I_m \ 0] \tilde{V}_k Y_r &= U_{k+1} X_{r+1} \begin{bmatrix} C_r \\ 0 \end{bmatrix}, & QQ^T \begin{bmatrix} U_{k+1} X_{r+1} \\ 0 \end{bmatrix} &= \tilde{V}_k Y_r [C_r \ 0] + \alpha_{k+1} \tilde{v}_{k+1} e_{k+1}^T X_{r+1}, \\ [0 \ I_p] \tilde{V}_k Y_r &= \hat{U}_k \hat{X}_r S_r, & QQ^T \begin{bmatrix} 0 \\ \hat{U}_k \hat{X}_r \end{bmatrix} &= \tilde{V}_k Y_r S_r + \check{\beta}_k \tilde{v}_{k+1} e_k^T \hat{X}_r, \end{aligned}$$

or

$$[I_m \ 0] \tilde{V}'_r = U'_{r+1} \begin{bmatrix} C_r \\ 0 \end{bmatrix}, \quad QQ^T \begin{bmatrix} U'_{r+1} \\ 0 \end{bmatrix} = \tilde{V}'_r [C_r \ 0] + \tilde{v}_{k+1} b_{r+1}^T, \quad (42)$$

$$[0 \ I_p] \tilde{V}'_r = \hat{U}'_r S_r, \quad QQ^T \begin{bmatrix} 0 \\ \hat{U}'_r \end{bmatrix} = \tilde{V}'_r S_r + \tilde{v}_{k+1} \hat{b}_r^T, \quad (43)$$

where $b_{r+1} = \alpha_{k+1} X_{r+1}^T e_{k+1}$ and $\hat{b}_r = \check{\beta}_k \hat{X}_r^T e_k$, while the orthonormal vector bases have been updated according to $U'_{r+1} = U_{k+1} X_{r+1}$, $\hat{U}'_r = \hat{U}_k \hat{X}_r$ and $\tilde{V}'_r = \tilde{V}_k Y_r$.

The bidiagonalization process continues with the updated vector bases and taking \tilde{v}_{k+1} as the next vector of the \tilde{V} basis. That is, algorithm 2 is run with the loop starting at $j = r+1$.

The process is illustrated graphically in fig. 3, in a similar way as was done for the SVD in fig. 2. This time, the pictures show the right Lanczos basis \tilde{V}_k , together with both bidiagonals J_k and \check{J}_k , and depict how these matrices evolve when the compression and extension are carried out. In the last panel (step 5), we can see how after restart both the upper and lower bidiagonals have the leading part with an arrowhead shape, with the spike pointing to the left in both cases.

Algorithm 3 summarizes the overall restarted procedure.

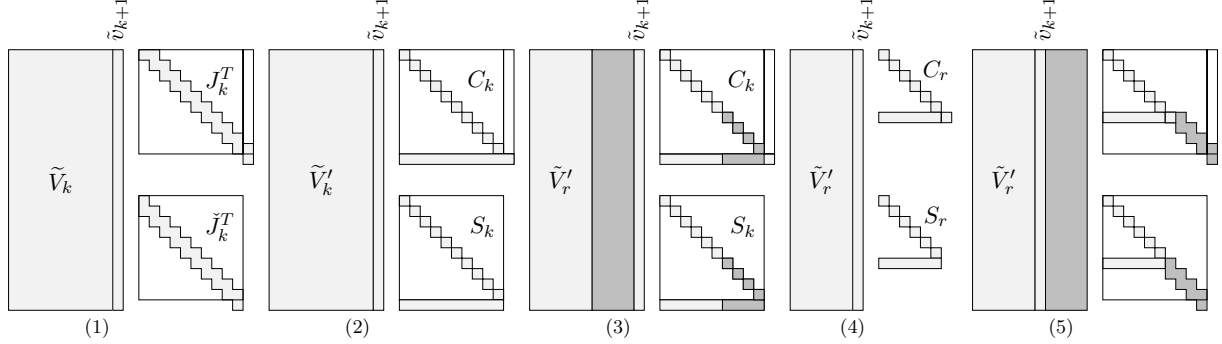


Figure 3: Illustration of the five steps of thick restart in GSVD: (1) initial Lanczos factorization of order k , (2) solve projected problem, (3) sort and check convergence, (4) truncate to factorization of order r , and (5) extend to a factorization of order k .

ALGORITHM 3: Thick-restarted joint Lanczos bidiagonalization for the GSVD

Input: Matrices $A \in \mathbb{R}^{m \times n}$, $B \in \mathbb{R}^{p \times n}$, unit-norm vector $u_1 \in \mathbb{R}^m$, maximum basis size k , restart size r , number of wanted generalized singular quadruples s , tolerance tol .

Output: Partial GSVD $U_s'^T A G_s = C_s$, $\widehat{U}_s'^T B G_s = S_s$.

- 1: Compute $\hat{\beta}_0, \tilde{v}_1, \alpha_1$ as in algorithm 2
 - 2: $j' = 0$
 - 3: **loop**
 - 4: **for** $j = j' + 1, j' + 2, \dots, k$ **do**
 - 5: Do step j of bidiagonalization (Lines 5–11 of algorithm 2)
 - 6: **end for**
 - 7: Compute the CS decomposition of $\{J_k, \check{J}_k\}$ as in (37)
 - 8: Reorder the CS decomposition according to c_i/s_i (in increasing or decreasing order)
 - 9: Declare convergence if $\sqrt{(\alpha_{k+1} e_{k+1}^T x_i)^2 + (\check{\beta}_k e_k^T \hat{x}_i)^2} < \text{tol}$ for $i = 1, \dots, s$, see section 3.2
 - 10: Compute $U_{r+1}', \widehat{U}_r', \tilde{V}_r', b_{r+1}$ and \hat{b}_r as in (42)-(43)
 - 11: Exit loop if converged, setting $g_j, j = 1, \dots, s$, as the solution to the least squares problem

$$\begin{bmatrix} A \\ B \end{bmatrix} g_j = \tilde{v}_j'$$
 - 12: $j' = r$
 - 13: **end loop**
-

3.2 Residual estimates

We now discuss a convergence criterion to be used in the computation of the partial GSVD with the method of section 3.1 to decide when an approximate generalized singular quadruple $(\tilde{\sigma}_i, \tilde{u}_i^A, \tilde{u}_i^B, \tilde{g}_i)$, with $\tilde{\sigma}_i = \tilde{c}_i/\tilde{s}_i$, can be considered converged. We must derive formulas for the estimates of residual norms, using the information obtained during the bidiagonalization, without expensive additional computation. The iteration stops when the number of converged solutions reaches the number requested by the user.

As in the case of the SVD (see section 2.4), there are two possible alternatives to define the residual associated to an approximate solution, in terms of either the cross product eigenproblem (14) or the cyclic eigenproblem (15),

$$r_i^{\text{CROSS}} = \tilde{s}_i^2 A^T A \tilde{g}_i - \tilde{c}_i^2 B^T B \tilde{g}_i, \quad (44)$$

$$r_i^{\text{CYCLIC,A}} = \begin{bmatrix} A \tilde{g}_i / \tilde{s}_i - \tilde{\sigma}_i \tilde{u}_i^A \\ A^T \tilde{u}_i^A - \tilde{\sigma}_i B^T B \tilde{g}_i / \tilde{s}_i \end{bmatrix}, \quad (45)$$

$$r_i^{\text{CYCLIC,B}} = \begin{bmatrix} B \tilde{g}_i / \tilde{c}_i - \tilde{\sigma}_i^{-1} \tilde{u}_i^B \\ B^T \tilde{u}_i^B - \tilde{\sigma}_i^{-1} A^T A \tilde{g}_i / \tilde{c}_i \end{bmatrix}. \quad (46)$$

The residual norm $\|r_i^{\text{CROSS}}\|_2$ was used by Zha [30], who showed, in the context of joint bidiagonalization with both bidiagonal matrices in upper form, that

$$\|(\tilde{s}_i^2 A^T A - \tilde{c}_i^2 B^T B) \tilde{g}_i\|_2 \leq \alpha_k \beta_k |e_k^T y_i| \|R\|_2,$$

where y_i is the i th right singular vector of the bidiagonal matrix J_k resulting from a k -step joint bidiagonalization process. In the case of joint bidiagonalization with lower-upper bidiagonal forms, the above inequality should be modified slightly,

$$\|(\tilde{s}_i^2 A^T A - \tilde{c}_i^2 B^T B) \tilde{g}_i\|_2 \leq \alpha_{k+1} \beta_{k+1} |e_k^T y_i| \|R\|_2. \quad (47)$$

The matrix R above is the triangular factor of the QR decomposition (5), so its 2-norm is not readily available, but it can be bounded by $\sqrt{m+p} \max\{\|A\|_\infty, \|B\|_\infty\}$.

The residual r_i^{CROSS} (44) does not take into account possible errors in left vectors $\tilde{u}_i^A, \tilde{u}_i^B$, so the residual $r_i^{\text{CYCLIC,A}}$ (45) may be more appropriate. This is the residual employed in the Jacobi-Davidson method [16]. It refers to \tilde{u}_i^A . Similarly, the residual $r_i^{\text{CYCLIC,B}}$ (46) stemming from the second cyclic eigenproblem in (15) refers to \tilde{u}_i^B . In the following, we define a convergence criterion that combines the two cyclic residuals so that both \tilde{u}_i^A and \tilde{u}_i^B are taken into consideration.

From the definition of the GSVD (26) we have

$$A g_i = c_i u_i^A, \quad (48)$$

$$B g_i = s_i u_i^B, \quad (49)$$

$$s_i A^T u_i^A = c_i B^T u_i^B. \quad (50)$$

Using (49) in (50), and in the same way using (48) in (50), we get

$$s_i^2 A^T u_i^A = c_i B^T B g_i, \quad (51)$$

$$\tilde{c}_i^2 B^T u_i^B = s_i A^T A g_i, \quad (52)$$

and we define a residual that accounts for these two relations, whose norm is

$$\|r^{\text{GSVD}}\|_2 = \sqrt{\|\tilde{s}_i^2 A^T \tilde{u}_i^A - \tilde{c}_i B^T B \tilde{g}_i\|_2^2 + \|\tilde{c}_i^2 B^T \tilde{u}_i^B - \tilde{s}_i A^T A \tilde{g}_i\|_2^2}. \quad (53)$$

We can derive bounds for this residual from the quantities computed in the joint bidiagonalization. From (40)-(41) we have

$$\begin{aligned} A\tilde{g}_i &= \tilde{c}_i\tilde{u}_i^A, & A^T\tilde{u}_i^A &= R^T(\tilde{c}_iR\tilde{g}_i + \alpha_{k+1}v_{k+1}e_{k+1}^T x_i), \\ B\tilde{g}_i &= \tilde{s}_i\tilde{u}_i^B, & B^T\tilde{u}_i^B &= R^T(\tilde{s}_iR\tilde{g}_i + \check{\beta}_k v_{k+1}e_k^T \hat{x}_i). \end{aligned} \quad (54)$$

Using (54) and taking into account that $\tilde{c}_i^2 + \tilde{s}_i^2 = 1$, the residual norm for (51) is

$$\begin{aligned} \|\tilde{s}_i^2 A^T \tilde{u}_i^A - \tilde{c}_i B^T B \tilde{g}_i\|_2 &= \|A^T \tilde{u}_i^A - \tilde{c}_i Z^T Z \tilde{g}_i\|_2 \\ &= \|A^T \tilde{u}_i^A - \tilde{c}_i R^T R \tilde{g}_i\|_2 = \|\alpha_{k+1} R^T v_{k+1} e_{k+1}^T x_i\|_2 \end{aligned}$$

with the bound

$$\|\tilde{s}_i^2 A^T \tilde{u}_i^A - \tilde{c}_i B^T B \tilde{g}_i\|_2 \leq \alpha_{k+1} |e_{k+1}^T x_i| \|R\|_2.$$

In fact, this is a bound for $\tilde{s}_i^2 \|r_i^{\text{CYCLIC,A}}\|$ for the cyclic residual (45), since the upper part of that residual is exactly zero due to the left relation in (54). Analogously, the residual associated to (52) verifies

$$\|\tilde{c}_i^2 B^T \tilde{u}_i^B - \tilde{s}_i A^T A \tilde{g}_i\|_2 \leq |\check{\beta}_k e_k^T \hat{x}_i| \|R\|_2,$$

which is related to $\tilde{c}_i^2 \|r_i^{\text{CYCLIC,B}}\|$. Combining the previous two bounds,

$$\|r^{\text{GSVD}}\|_2 \leq \sqrt{(\alpha_{k+1} e_{k+1}^T x_i)^2 + (\check{\beta}_k e_k^T \hat{x}_i)^2} \|R\|_2. \quad (56)$$

It is interesting to see that $\|r^{\text{GSVD}}\|_2$ is equal to the residual norm of (50). Using (48) and (49) we have

$$\begin{aligned} \|\tilde{s}_i^2 A^T \tilde{u}_i^A - \tilde{c}_i B^T B \tilde{g}_i\|_2 &= \|\tilde{s}_i^2 A^T \tilde{u}_i^A - \tilde{c}_i \tilde{s}_i B^T \tilde{u}_i^B\|_2 = \tilde{s}_i \|\tilde{s}_i A^T \tilde{u}_i^A - \tilde{c}_i B^T \tilde{u}_i^B\|_2, \\ \|\tilde{c}_i^2 B^T \tilde{u}_i^B - \tilde{s}_i A^T A \tilde{g}_i\|_2 &= \|\tilde{c}_i^2 B^T \tilde{u}_i^B - \tilde{s}_i \tilde{c}_i A^T \tilde{u}_i^A\|_2 = \tilde{c}_i \|\tilde{c}_i B^T \tilde{u}_i^B - \tilde{s}_i A^T \tilde{u}_i^A\|_2, \end{aligned}$$

and

$$\|r^{\text{GSVD}}\|_2 = \|\tilde{s}_i A^T \tilde{u}_i^A - \tilde{c}_i B^T \tilde{u}_i^B\|_2.$$

As a summary, our criterion to accept a computed generalized singular quadruple as converged during the restart of the joint bidiagonalization is $\sqrt{(\alpha_{k+1} e_{k+1}^T x_i)^2 + (\check{\beta}_k e_k^T \hat{x}_i)^2} < \mathbf{tol}$, where \mathbf{tol} is the user-defined tolerance. According to (56), this can be considered a criterion relative to the norm of the problem matrices.

3.3 Using a scale factor

We have implemented an option for scaling one of the matrices, as this may be beneficial for convergence in some cases. When the user specifies a scale factor γ , the method is applied to the pair $\{A, \gamma B\}$ instead of $\{A, B\}$. As a consequence, the algorithm works with a modified coefficient matrix for the least squares problem,

$$Z_\gamma := \begin{bmatrix} A \\ \gamma B \end{bmatrix} = \begin{bmatrix} Q_{A,\gamma} \\ Q_{B,\gamma} \end{bmatrix} R_\gamma,$$

where $Q_{A,\gamma}$ and $Q_{B,\gamma}$ are different from those obtained without scaling.

If we use $(c_i, s_i, u_i^A, u_i^B, g_i)$ to denote the solution for the pair $\{A, B\}$ as in (4), we can write the relations for the scaled problem as

$$A(\omega_i g_i) = (\omega_i c_i) u_i^A, \quad \gamma B(\omega_i g_i) = (\gamma \omega_i s_i) u_i^B, \quad (57)$$

for certain weights ω_i , so after solving (57) we can retrieve the solution of the original problem (4) by multiplying the generalized singular values σ_i by γ and also multiplying the g_i vectors by ω_i^{-1} , which can be obtained from the relation

$$\omega_i^2 c_i^2 + \gamma^2 \omega_i^2 s_i^2 = 1, \quad \omega_i^{-1} = \sqrt{c_i^2 + \gamma^2 s_i^2},$$

where c_i, s_i , corresponding to the original problem, can be computed from σ_i .

The convergence of the joint Lanczos bidiagonalization for the GSVD is determined by the convergence of the Lanczos bidiagonalization of Q_A to approximate the values c_i (or equivalently, the bidiagonalization of Q_B to approximate the values s_i). As [25] shows, the relative gap of the first two eigenvalues, $\rho_1 = (\lambda_1 - \lambda_2)/(\lambda_2 - \lambda_n)$, with $\lambda_i = c_i^2$ in our case, is of key importance for the convergence rate of Lanczos to approximate λ_1 , with convergence increasing as ρ_1 grows. Thus, it is interesting to analyze how ρ_1 is affected by scaling. The relative gap of the scaled problem is $\rho'_1 = (c_1'^2 - c_2'^2)/(c_2'^2 - c_n'^2)$, with $c_i' = \omega_i c_i$, according to (57). The ratio ρ'_1/ρ_1 is

$$\frac{\rho'_1}{\rho_1} = \frac{(c_1'^2 - c_2'^2)(c_2^2 - c_n^2)}{(c_2'^2 - c_n'^2)(c_1^2 - c_2^2)} = \frac{c_n^2 + \gamma^2(1 - c_n^2)}{c_1^2 + \gamma^2(1 - c_1^2)} = \frac{\omega_1^2}{\omega_n^2}.$$

As γ grows, ρ'_1/ρ_1 will also grow, tending to $(1 - c_n^2)/(1 - c_1^2)$, and favoring convergence of the scaled problem. This can be seen in fig. 4 (left), which shows the value of ρ'_1/ρ_1 vs γ for $\sigma_n = c_n/s_n = 10^{-3}$ and different values of $\sigma_1 = c_1/s_1$. Clearly, problems with large σ_1 should benefit the most from scaling. The figure suggests that values of γ near σ_1 should be good for convergence (but of course σ_1 is unknown a priori).

On the other hand, if we want to compute the smallest generalized singular value $\sigma_n = c_n/s_n$, the relative gap of interest is $\hat{\rho}_n = (c_{n-1}^2 - c_n^2)/(c_1^2 - c_{n-1}^2)$, with the corresponding ratio

$$\frac{\hat{\rho}'_n}{\hat{\rho}_n} = \frac{(c_{n-1}'^2 - c_n'^2)(c_1^2 - c_{n-1}^2)}{(c_1'^2 - c_{n-1}'^2)(c_{n-1}^2 - c_n^2)} = \frac{\omega_n^2}{\omega_1^2}.$$

In this case, the ratio will grow as γ decreases, tending to c_1^2/c_n^2 , as can be seen in fig. 4 (right).

Section 5 includes some results comparing different values of γ . A good choice of γ is application-dependent. An in-depth theoretical analysis of the impact of scaling on performance is out of the scope of this paper, as it depends on many factors. On one hand, a suitable value of γ can improve the relative separation of the target singular values of $Q_{A,\gamma}$ and $Q_{B,\gamma}$, but on the other hand this may bring an increase of the condition number of matrix Z_γ with the consequent negative effects (especially if using an iterative least squares solver such as LSQR).

3.4 One-sided orthogonalization

When the thick restart technique was introduced for the SVD in section 2.5, we pointed out that the loss of orthogonality among Lanczos vectors can be avoided by means of full orthogonalization, that is, enforcing the full orthogonality of both left and right Lanczos bases via explicit orthogonalization. In practice, lines 3 and 5 of algorithm 1 are replaced with $p_j = \text{orthog}(Aq_j, P_{j-1})$ and $q_{j+1} = \text{orthog}(A^T p_j, Q_j)$. However, Simon and Zha [27] showed that it is not necessary to explicitly orthogonalize both bases, and it is enough with orthogonalizing one of them since the level of orthogonality of left and right Lanczos vectors go hand

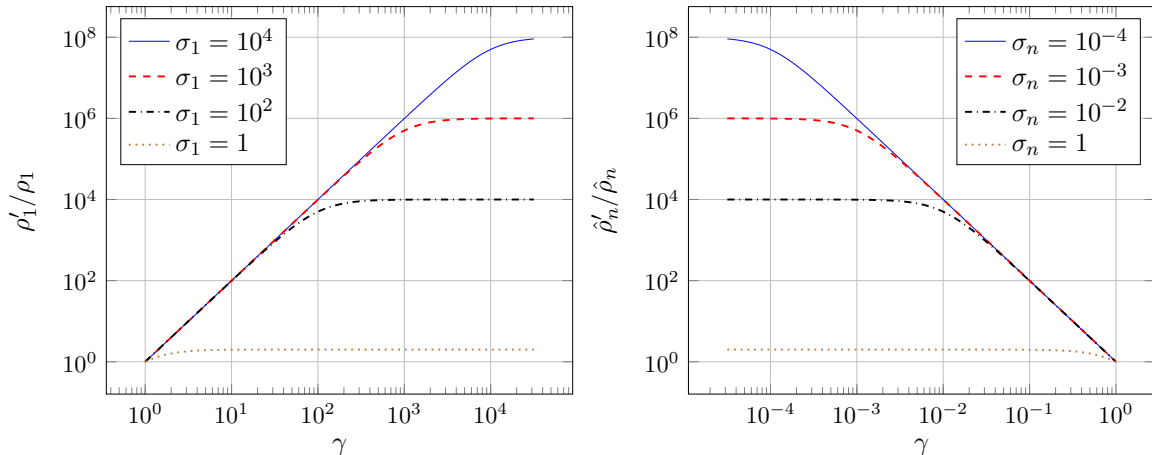


Figure 4: Left: relative gap ratio ρ'_1/ρ_1 vs scale factor γ , for $\sigma_n = 10^{-3}$ and different values of σ_1 . Right: relative gap ratio $\hat{\rho}'_n/\hat{\rho}_n$ vs scale factor γ , for $\sigma_1 = 100$ and different values of σ_n .

in hand. This technique is called one-sided orthogonalization, and is implemented in SLEPc's thick-restart Lanczos solver for the SVD [15], reducing the cost of each iteration significantly.

The one-sided orthogonalization technique can also be applied to the GSVD case. In Kilmer's joint bidiagonalization (algorithm 2), lines 5, 7 and 9 involve a full orthogonalization that would be implemented with a call to `orthog()`. However, two of these three orthogonalizations can be avoided, that is, instead of explicitly orthogonalizing against the full basis, just a local orthogonalization with the previous vector is done. In particular, we have found that it is enough to explicitly orthogonalize the U_{k+1} basis (line 7). This saves about two thirds of the orthogonalization cost, as will be illustrated in the computational results of section 5.

One-sided orthogonalization in the context of joint Lanczos bidiagonalization is discussed in [19], where the authors show that it is sufficient to explicitly orthogonalize U_{k+1} and V_k , provided that the bidiagonal matrix J_k does not become too ill-conditioned. Note that our one-sided orthogonalization strategy is more aggressive, as it orthogonalizes just one basis instead of two. That is why in our solver one-sided orthogonalization is an option that the user can activate, but by default full orthogonalization of the three bases is carried out. However, in our tests we have not found any situation where the one-sided variant leads to large residual norms or a bad level of orthogonality of the computed bases.

If we consider the overall computational cost, the saving from one-sided orthogonalization may be modest, since each iteration of the loop of algorithm 2 performs a least squares solve at line 9, whose cost is usually much higher, especially if using the LSQR iterative method. See results in section 5.

4 Details of the implementation in SLEPc

We now discuss a few relevant details of our implementation, with which the results shown in section 5 have been obtained. The implementation is included in one of the solvers of SLEPc, the Scalable Library for Eigenvalue Problem Computations [14]. We first give an overview of this library, before going into the details.

SLEPc is a parallel library intended for solving large-scale eigenvalue problems, mainly by iterative methods, that is, in cases where only part of the spectrum is required. It consists of several modules, each one for a different type of problem, including linear eigenproblems, polynomial eigenproblems, general nonlinear eigenproblems, and singular-value-type decompositions.

The latter module is called **SVD** and is the one relevant for this work.

SLEPc can be seen as an extension of PETSc, the Portable, Extensible Toolkit for Scientific Computation [4]. PETSc provides a lot of functionality related to data structures and solvers useful for large-scale scientific applications modeled by partial differential equations. Apart from the basic data objects for working with matrices and vectors, the only PETSc modules that are relevant for this work are those implementing iterative methods for linear systems of equations (**KSP**) and preconditioners (**PC**).

The model of parallelism of PETSc/SLEPc is message-passing (MPI), where every object is created with respect to an MPI communicator, implying that certain operations are carried out collectively by all processes belonging to that communicator. A second level of parallelism is also available to further accelerate the local computations either via CPU threads or by launching kernels to a GPU, but we do not consider them in this paper.

The solver modules are essentially a collection of solvers with a common user interface, where the user can choose the solver to be employed. This selection can be done at run time via command-line options, which confers a lot of flexibility by allowing also to specify solver parameters such as the dimension of the subspace, the tolerance, and many more. In the case of the **SVD** module, it contains a number of solvers, from which we highlight the following:

- **cross**. This solver originally contained a gateway for computing the SVD via the linear eigenvalue problem module, in particular with the equivalent cross product matrix eigenproblem, (11) or (12). In this work, we have extended this for the GSVD via the equivalent eigenproblem (14).
- **cyclic**. Similarly to the previous one, this solver had code for the SVD formulated via the cyclic eigenproblem (13), and we have extended it for the GSVD using the equivalent cyclic eigenproblems (15).
- **trlanczos**. This is the thick-restart Lanczos solver. The implementation for the SVD is described in [26]. The extension to the GSVD, following the methodology detailed in section 3, constitutes the main contribution of this paper.

At the core of the thick-restart Lanczos solver is the lower-upper² joint bidiagonalization of algorithm 2. One of the main operations in this algorithm is the orthogonalization of vectors, which in SLEPc is carried out with an iterated classical Gram-Schmidt variant that is both efficient in parallel and numerically stable [13]. Another notable operation is the expansion of the \tilde{V} Lanczos basis, which implies the solution of the least squares problem (36). This is done using PETSc’s functionality, as described next.

PETSc allows combining iterative methods from **KSP** with preconditioners from **PC**, for instance **gmres** and **jacobi**. Direct linear solvers can be used with a special **KSP** that means precondition only, e.g., **preonly** and **lu**. There are a limited number of instances of **KSP** and **PC** that can handle rectangular matrices, so the possibilities for least squares problems are:

- A purely iterative method, i.e., without preconditioning, via the **KSP** solver **lsqr** that implements the LSQR method [24], or the **cgls** method, which is equivalent to applying the conjugate gradients on the normal equations.
- A direct method, with **preonly** and **qr**. This requires installing PETSc together with SuiteSparse, which implements a sparse QR factorization [7].

²We have also implemented the upper-upper variant (Zha’s method), including thick restart, but we do not consider this here to keep the presentation short.

- A combination of the two, i.e., `lsqr` and `qr`. Since `qr` is a direct method, the `lsqr` method will finish in just one iteration. Note that LSQR requires that the preconditioner is built for the normal equations matrix $Z^T Z$, which means that in the case of `qr` the preconditioner application will consist in a forward triangular solve followed by a backward triangular solve with R , the computed triangular factor. Even though the number of iterations is one, due to how the method is implemented the number of preconditioner applications is two, but still this is usually cheaper than `preonly` with `qr` because the latter needs applying the orthogonal factor of the QR decomposition, which is avoided with `lsqr`.
- The iterative method `lsqr` with a parallel preconditioner for the normal equations. One possible parallel preconditioner is block Jacobi (`bjacobi`), a simple domain-decomposition preconditioner where each process applies a local preconditioner built from the block-diagonal part of the distributed matrix. In our case, the local preconditioner can be `qr`. A more effective preconditioner is algebraic multigrid as implemented in HyPre [10] or an advanced domain decomposition scheme as implemented in HPDDM [21]. The latter has been specifically adapted for the case of the normal equations following the method in [6].

We will consider `lsqr` with or without preconditioner. The former case requires that matrix Z is built explicitly, by stacking the user matrices A and B , while the unpreconditioned `lsqr` can operate with A and B independently. Hence, we have added a user parameter `explicitmatrix` that can be turned on if necessary. This option applies also to the `cross` and `cyclic` solvers to explicitly build the matrices of (14) and (15), which is necessary in the case that a direct linear solver is to be used in the solution of the eigenproblem, e.g., to factorize matrix $B^T B$.

Apart from the joint bidiagonalization of algorithm 2, the main ingredient of the solver is the thick restart discussed in section 3. In SLEPc, the small-sized dense projected problem is handled within an auxiliary object called `DS`, with operations to solve the projected problem, sort the computed solution according to a certain criterion, and truncate it to a smaller size, among other. For the GSVD, we have implemented the computation of the CS decomposition (37) using LAPACK's subroutine `_GGSVD3`, and the truncation operation that manages the arrowhead shapes in fig. 3 using a compact storage.

A common parameter in all SLEPc solvers is `ncv`, the number of column vectors, that is, the maximum allowed dimension of the subspaces. In SVD-type computations, the user can also choose whether to compute the largest (default) or smallest (generalized) singular values and vectors. The user interface of the GSVD thick-restart solver includes three additional parameters: the scale factor, discussed in section 3.3, a flag to enable one-sided orthogonalization, discussed in section 3.4, and the restart parameter, indicating the proportion of basis vectors that must be kept after restart (the default is 50%).

A final comment is about locking. The absolute value of the spikes of arrows in fig. 3 are precisely the residual bounds used in the convergence criterion (56). As soon as the generalized singular quadruples converge, the leading values of these spikes become small (below the tolerance). Then one could set these values to zero explicitly, with the consequent decoupling from the rest of the bidiagonalization. This is called locking, a form of deflation in which the converged solutions are used in the orthogonalization but are excluded from the rest of operations. In our solver, locking is active by default, but the user can deactivate it so that the full bidiagonalization is updated at restart (including converged vectors). All results discussed in next section use locking.

Table 1: Description of the test problems used in the computational experiments: number of rows m and columns n of A , number of rows p of B , number of requested generalized singular values `nsv`, whether largest or smallest generalized singular values are wanted, and the first computed value.

name	m	n	p	nsv	which	first value
diagonal	500000	500000	500000	20	largest	$\sigma_1 = 0.57735$
invinterp	262144	262144	524288	20	largest	$\sigma_1 = 25701.6$
hardesty2	626256	303645	303645	20	largest	$\sigma_1 = 53990.8$
3elt	4720	4720	4721	5	largest	$\sigma_1 = 8727.4$
gemat12	4929	4929	4930	5	largest	$\sigma_1 = 47738$
onetone1	36057	36057	36058	5	smallest	$\sigma_n = 3.44 \cdot 10^{-4}$

5 Computational results

In this section we present results of some computational experiments to assess the performance of the solvers in terms of accuracy, convergence, and parallel scalability. The executions have been carried out on the Tirant III computer, which consists of 336 computing nodes, each of them with two Intel Xeon SandyBridge E5-2670 processors (16 cores each) running at 2.6 GHz with 32 GB of memory, connected with an Infiniband network. We allocated 4 MPI processes per node at most. The presented results correspond to SLEPc version 3.18, together with PETSc 3.18³, SuiteSparse 5.13, hypre 2.25 and MUMPS 5.5. All software has been compiled with Intel C and Fortran compilers (version 18) and Intel MPI.

Table 1 lists the problems used in the experiments, summarizing some properties and parameters. Here is a short description of the problems:

- The **diagonal** problem is taken from [30, Example 1], but with larger dimension. The problem matrices are computed as $A = CD$ and $B = SD$, where $C = \text{diag}(c_i)$ with $c_i = (n - i + 1)/2n$, $S = \sqrt{I - C^2}$, and $D = \text{diag}(d_i)$ with $d_i = [4i/n] + r_i$ where r_i is a random number uniformly distributed on $[0, 1]$.
- The **invinterp** case corresponds to the inverse interpolation problem of IR Tools [11, §3.2], intended to test iterative regularization methods for linear inverse problems. The GSVD can be used in this context. In this case, the A matrix comes from the interpolation relations of n points at random locations with respect to a 2D regular grid of side \sqrt{n} , and B is the regularization matrix. In our case, for matrix B we use the last case listed in [11, §4.2] (2D Laplacian with zero derivative enforced on one of the boundaries) except that we do not compute the compact QR decomposition of this matrix.
- In the **3elt**, **gemat12** and **onetone1** problems, the A matrix is the matrix with the same name taken from the SuiteSparse matrix collection [8], while the B matrix is a bidiagonal matrix with one more row than columns and values -1 and 1 on the subdiagonal and diagonal, respectively. The **hardesty2** matrix also belongs to the SuiteSparse matrix collection, but instead of using it with a bidiagonal matrix, we take the bottom square block as matrix B and the remaining top rows as matrix A .

All results in this section are obtained with the `explicitmatrix` flag set, except for the **diagonal**, **3elt**, **gemat12** and **onetone1** problems when using LSQR without a preconditioner. The stopping tolerance for LSQR is 10^{-10} . Table 2 illustrates the performance of our solver with

³With a patch required to improve the performance when using the `hypre` preconditioner with `lsqr`, that will be included in PETSc 3.19.

Table 2: Computational results for the first three test cases, solved sequentially and in parallel (with 16 MPI processes), using a sparse QR factorization or the LSQR iterative method for the least squares solves, respectively. We show the scale factor γ , the number of Lanczos restarts, the total number of iterations of the linear solver, the execution time in seconds, and the maximum relative residual norm of all computed solutions.

test problem	LS solver	processes	γ	restarts	linear its	time	residual
diagonal	QR	1	1	763	12479	2847	$6 \cdot 10^{-9}$
invinterp	QR	1	50	69	1232	585	$2 \cdot 10^{-9}$
hardesty2	QR	1	1000	3	102	81	$6 \cdot 10^{-11}$
diagonal	LSQR	16	1	818	701867	489	$6 \cdot 10^{-9}$
invinterp	LSQR-hypre	16	50	65	41049	407	$1 \cdot 10^{-7}$
hardesty2	LSQR-hypre	16	1000	4	26813	218	$3 \cdot 10^{-10}$

the first three test cases. In sequential runs we use the sparse QR factorization to solve the least squares problems, and in parallel we employ LSQR, which may need a lot of iterations (the `diagonal` and `invinterp` problems can be solved without preconditioner, but in `hardesty2` a preconditioner is required). From the table, we can see that both `invinterp` and `hardesty2` need more time in parallel than sequentially, because LSQR is slow (this is also related to the scale factor as discussed below). Still, parallelism allows solving very large problems where computing a sequential sparse QR is not viable.

To assess the accuracy of the computed generalized singular quadruples, we use the residual norm (53) relative to the norm of the stacked matrix (5), $\|r^{\text{GSVD}}\|_2 / \|Z\|_\infty$. The default tolerance for the thick-restart Lanczos solver is 10^{-8} , and we see in table 2 that the relative residual norm is below the tolerance in all cases except for `invinterp` with LSQR. This can be fixed by requesting a more stringent tolerance for the LSQR stopping criterion, otherwise a bad accuracy of the inner iteration prevents attaining the requested accuracy in the outer one.

In the case of a sparse QR factorization, the value of the total number of iterations of the linear solver in table 2 can be interpreted as the number of least squares problems that need to be solved. To understand this value, we have to take into account that the default value of `ncv` (number of column vectors) is equal to $\max\{2 \cdot \text{nsv}, 10\}$, that is, 40 in the case of the test problems analyzed in table 2. In addition to the least squares problems required during the Lanczos iteration, the postprocessing to obtain the final right singular vectors $g_i = R^{-1}w_i$ requires additional least squares solves.

If we wanted to compare the performance of our thick-restarted GSVD solver (algorithm 3) with respect to a non-restarted solver (the algorithms in [30] and [18], for instance), one possibility would be to emulate the latter by using the restarted solver with a sufficiently large basis size (`ncv`) so that restart is never required. We have carried out this comparison with the `invinterp` problem with a sparse QR for the least squares (second line of table 2), using bases of `ncv=765` vectors⁴. Of course, in terms of memory use, the restarted solver is much cheaper since each of the three vector bases need to store only 40 vectors, compared to the 765 vectors of the non-restarted solver. But it is also cheaper in terms of computational cost, as shown in fig. 5. Clearly the orthogonalization cost blows up in the non-restarted variant. The cost associated with solving least squares problems increases in the thick-restart case, because the total number of performed least squares solves is 1232, larger than 789 required for the non-restarted version. Overall, the thick-restart solver takes less than half the time of the non-restarted one.

The scale factor discussed in section 3.3 may have a significant impact on the performance

⁴This value has been chosen *a priori*, but an actual implementation of a non-restarted solver should have to check convergence at every Lanczos step, which would increase the overall cost.

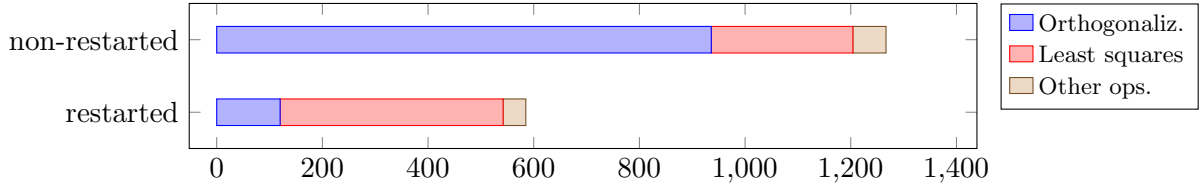


Figure 5: Comparison of the execution time (in seconds) of the non-restarted and thick-restarted methods when solving the `invinterp` problem with a sparse QR for the least squares using 1 MPI process. Other operations include the initial computation of the QR factorization, the solution of the projected problem (37) and the update of bases (42)-(43) required at restart (and at the end of the algorithm).

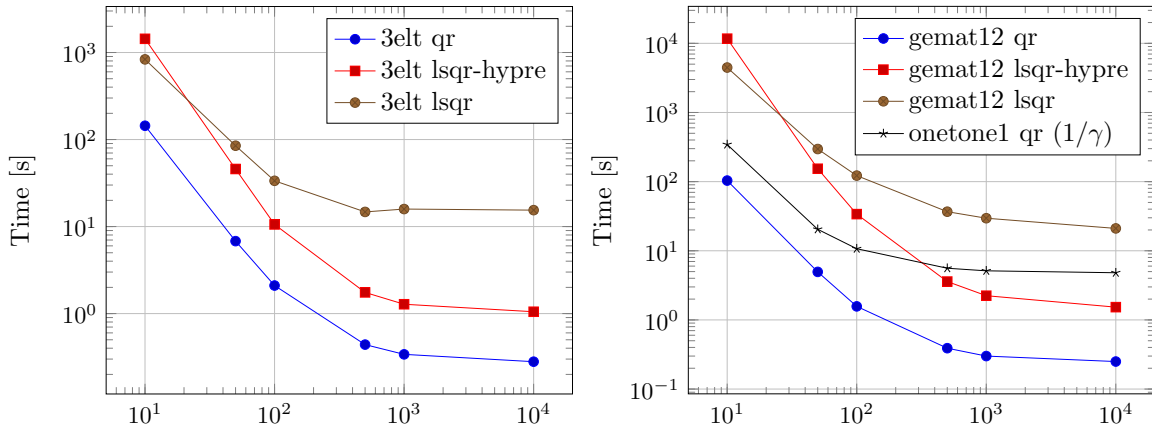


Figure 6: Execution time (in seconds) with different scale factors, for matrices `3elt` (left), `gemat12` and `onetone1` (right).

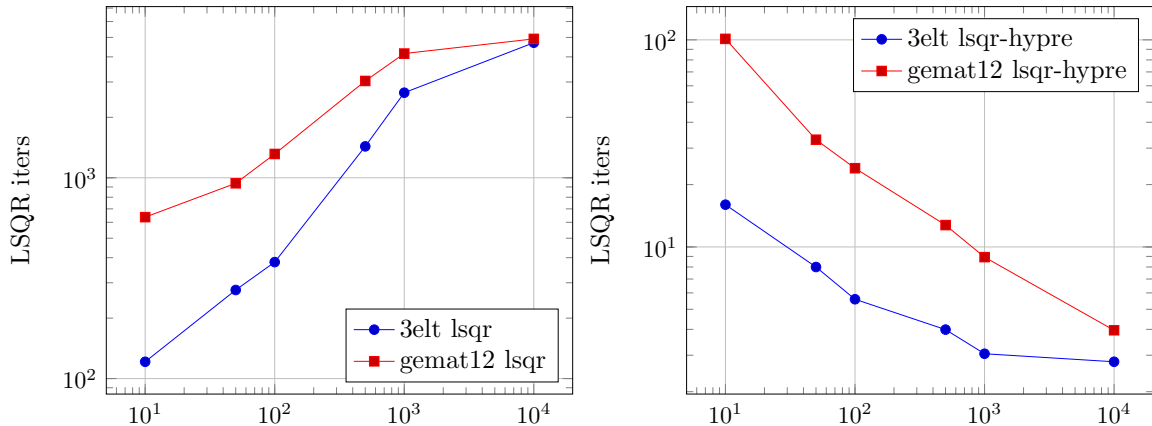


Figure 7: Average number of LSQR iterations per least squares solve for 3elt and gemat12 with different scale factors, considering no preconditioner (left) or hypre preconditioner (right).

of the thick-restart Lanczos solver, as it has an influence on the number of Lanczos restarts as well as the number of iterations needed by LSQR. Figure 6 compares the execution time of the last problems in table 1 when the scale factor is changed, and using three different methods to solve the least squares problem: sparse QR, unpreconditioned LSQR and LSQR with an algebraic multigrid preconditioner from Hypre. We can draw several conclusions. First, in all these problems scaling is beneficial, and execution time is reduced whenever the scale factor γ is increased, up to a point where it stabilizes. This is also true, but with the reciprocal of γ , if the smallest generalized singular values are computed (`onetone1` problem). Second, in these problems it is much cheaper to use a sparse QR factorization for the least squares problems, compared to solving them with LSQR (either with or without preconditioning) as the latter may require many iterations (it does not converge in the `onetone1` problem). Still, LSQR is currently necessary for parallel runs, and in fig. 7 we study how the number of iterations of LSQR changes with respect to the scale factor. As the scale factor increases, the unpreconditioned LSQR method has more difficulties to converge, but the preconditioned LSQR improves its convergence speed.

Figure 8 shows the execution time of the thick-restart Lanczos solver compared with the cross and cyclic solvers discussed in section 2.2. In all cases we use a direct method for the linear solves (SuiteSparse for Lanczos and MUMPS for cross and cyclic). There is no clear winner, but take into account that in Lanczos we are using the scale factor γ that gave the smallest time in our tests for each problem, otherwise the Lanczos solver is not competitive in general. However, it is worth noting that for the `hardesty2` problem, the Lanczos solver is the only one that provides a suitable solution in terms of the residual. In this case, the matrix $B^T B$ in the cross and cyclic methods is singular and, because the generalized symmetric-definite Lanczos eigensolver fails, one has to solve the equivalent eigenproblem as non-symmetric, resulting in much lower accuracy ($\approx 1 \cdot 10^{-4}$), compared to the Lanczos GSVD solver ($\approx 6 \cdot 10^{-11}$). In the other cases, the relative residual norm of the computed solutions is similar in all solvers.

We conclude this section by analyzing parallel performance. Figure 9 plots the parallel execution time of the Lanczos solver for the `diagonal` problem with up to 64 MPI processes, using unpreconditioned LSQR. We can see that the scaling is very good, close to the ideal one. The figure shows the one-sided variant together with the default one (two-sided). The one-sided variant is always faster, but the difference is not too significant because orthogonalization amounts to only a modest percentage of the overall cost. To better appreciate the gain of one-sided orthogonalization, the right panel of fig. 9 shows only the time of the orthogonalization,

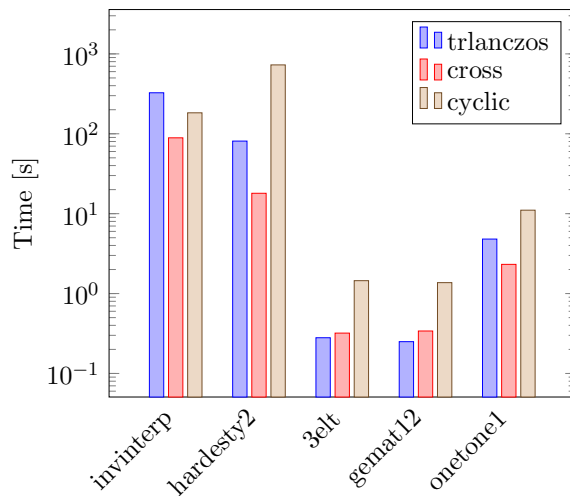


Figure 8: Comparing the thick-restart Lanczos solver (using the best scale parameter γ and sparse QR for the least squares problems) with the cross and cyclic solvers (using MUMPS for the linear solves).

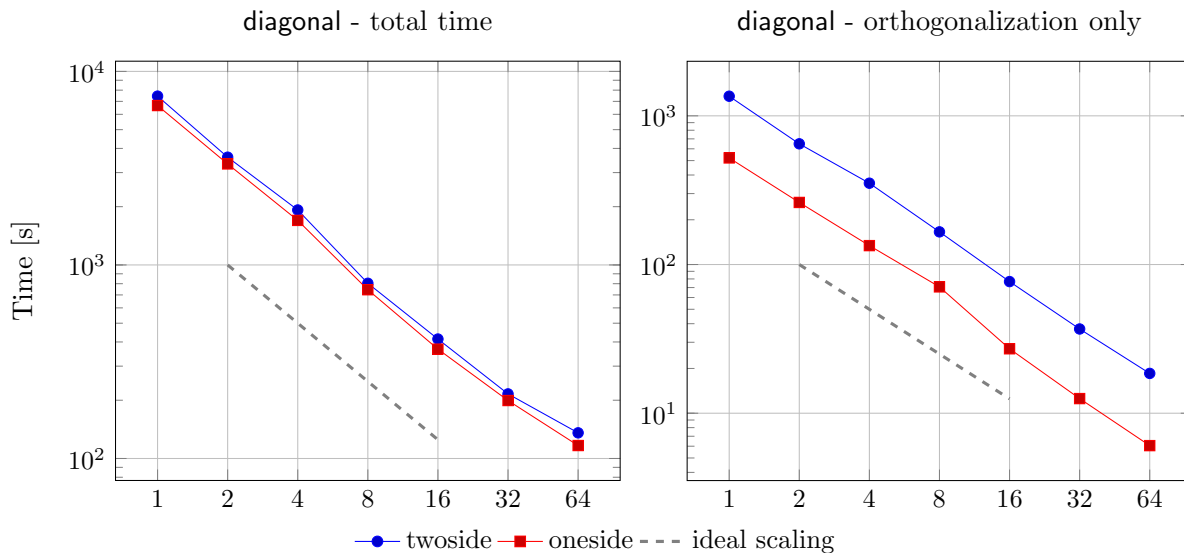


Figure 9: Execution time (in seconds) with up to 64 MPI processes for the diagonal problem, solved with thick-restart Lanczos using one-sided or two-sided orthogonalization. The left plot shows the total time, while the right one accounts only for the time of orthogonalization.

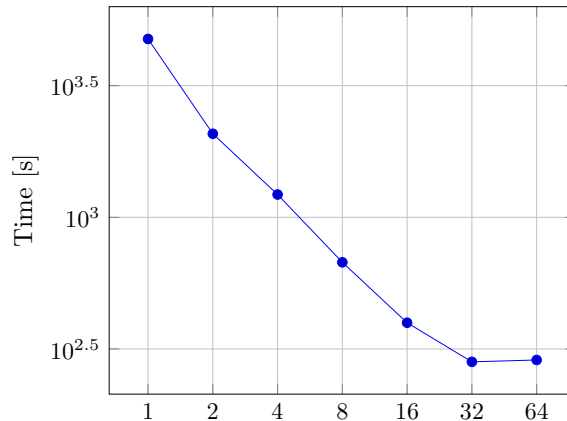


Figure 10: Execution time (in seconds) with up to 64 MPI processes for the `invinterp` problem, solved with thick-restart Lanczos and `hypre`-preconditioned LSQR.

with a factor of about 2.5 improvement of the one-sided scheme with respect to the default.

The `diagonal` problem is very favorable for parallel computing, as the matrix-vector product is trivially parallelizable. On the other extreme, the `invinterp` problem has a very disadvantageous sparsity pattern (nonzeros located at random positions), so the speedup shown in fig. 10 is good up to 32 MPI processes, but stagnates afterwards.

6 Concluding remarks

We have developed a thick restart mechanism for the joint Lanczos bidiagonalization to compute a partial GSVD of a large-scale matrix pair. This is a very important piece to make the solver usable in the context of real applications. We have developed a fully-fledged implementation in the SLEPc library, that in addition to the restart, includes other interesting features such as one-sided orthogonalization, scaling, or locking. The solver is very flexible, in the sense that the user can indicate at run time whether the associated least squares problems must be solved with a direct or iterative method, as well as specify many other settings such as the dimension of the Krylov subspace or the scale factor.

We have conducted a number of computational experiments, showing that our solver is numerically robust, computationally efficient and scalable in parallel runs. If an appropriate scale factor is used, the performance of Lanczos method is on a par with that of the cross and cyclic solvers for the GSVD, which we have also developed during this work.

Acknowledgements The authors would like to thank P. Jolivet for useful suggestions about parallel preconditioning in PETSc. The computational experiments of section 5 were carried out on the supercomputer Tirant III belonging to Universitat de València.

References

- [1] E. Anderson, Z. Bai, C. Bischof, L. S. Blackford, J. Demmel, J. Dongarra, J. Du Croz, A. Greenbaum, S. Hammarling, A. McKenney, and D. Sorensen. *LAPACK Users' Guide*. Society for Industrial and Applied Mathematics, Philadelphia, PA, third edition, 1999.
- [2] James Baglama and Lothar Reichel. Augmented implicitly restarted Lanczos bidiagonalization methods. *SIAM J. Sci. Comput.*, 27(1):19–42, 2005.

- [3] Z. Bai, J. Demmel, J. Dongarra, A. Ruhe, and H. van der Vorst, editors. *Templates for the Solution of Algebraic Eigenvalue Problems: A Practical Guide*. Society for Industrial and Applied Mathematics, Philadelphia, PA, 2000.
- [4] S. Balay, S. Abhyankar, M. F. Adams, J. Brown S. Benson, P. Brune, K. Buschelman, E. M. Constantinescu, L. Dalcin, A. Dener, V. Eijkhout, J. Faibussowitsch, W. D. Gropp, V. Hapla, T. Isaac, P. Jolivet, D. Karpeev, D. Kaushik, M. G. Knepley, F. Kong, S. Kruger, D. A. May, L. Curfman McInnes, R. Tran Mills, L. Mitchell, T. Munson, J. E. Roman, K. Rupp, P. Sanan, J. Sarich, B. F. Smith, S. Zampini, H. Zhang, H. Zhang, and J. Zhang. *PETSc/TAO Users Manual Revision 3.18*, 2022. Argonne Technical Memorandum ANL-21/39.
- [5] C. Campos and J. E. Roman. Restarted Q-Arnoldi-type methods exploiting symmetry in quadratic eigenvalue problems. *BIT*, 56(4):1213–1236, 2016.
- [6] H. Al Daas, P. Jolivet, and J. A. Scott. A robust algebraic domain decomposition preconditioner for sparse normal equations. *SIAM J. Sci. Comput.*, 44(3):A1047–A1068, 2022.
- [7] T. A. Davis. Algorithm 915, SuiteSparseQR: Multifrontal multithreaded rank-revealing sparse QR factorization. *ACM Trans. Math. Software*, 38(1):1–22, 2011.
- [8] T. A. Davis and Y. Hu. The University of Florida Sparse Matrix Collection. *ACM Trans. Math. Software*, 38(1):1:1–1:25, 2011.
- [9] A. Edelman and Y. Wang. The GSVD: Where are the ellipses?, matrix trigonometry, and more. *SIAM J. Matrix Anal. Appl.*, 41(4):1826–1856, 2020.
- [10] Robert D. Falgout and Ulrike Meier Yang. hypre: A library of high performance preconditioners. In Peter M. A. Sloot, Chih Jeng Kenneth Tan, Jack Dongarra, and Alfons G. Hoekstra, editors, *Computational Science - ICCS 2002, International Conference, Amsterdam, The Netherlands, April 21-24, 2002. Proceedings, Part III*, volume 2331 of *Lect. Notes Comp. Sci.*, pages 632–641. Springer, 2002.
- [11] S. Gazzola, P. C. Hansen, and J. G. Nagy. IR Tools: a MATLAB package of iterative regularization methods and large-scale test problems. *Numer. Algorithms*, 81(3):773–811, 2018.
- [12] G. H. Golub and C. F. van Loan. *Matrix Computations*. The Johns Hopkins University Press, Baltimore, MD, third edition, 1996.
- [13] V. Hernandez, J. E. Roman, and A. Tomas. Parallel Arnoldi eigensolvers with enhanced scalability via global communications rearrangement. *Parallel Comput.*, 33(7–8):521–540, 2007.
- [14] V. Hernandez, J. E. Roman, and V. Vidal. SLEPc: A scalable and flexible toolkit for the solution of eigenvalue problems. *ACM Trans. Math. Software*, 31(3):351–362, 2005.
- [15] Vicente Hernandez, Jose E. Roman, and Andres Tomas. A robust and efficient parallel SVD solver based on restarted Lanczos bidiagonalization. *Electron. Trans. Numer. Anal.*, 31:68–85, 2008.
- [16] M. E. Hochstenbach. A Jacobi–Davidson type method for the generalized singular value problem. *Linear Algebra Appl.*, 431(3-4):471–487, 2009.

- [17] J. Huang and Z. Jia. On choices of formulations of computing the generalized singular value decomposition of a large matrix pair. *Numer. Algorithms*, 87(2):689–718, 2020.
- [18] Z. Jia and H. Li. The joint bidiagonalization process with partial reorthogonalization. *Numer. Algorithms*, 88(2):965–992, 2021.
- [19] Z. Jia and H. Li. The joint bidiagonalization method for large GSVD computations in finite precision. *SIAM J. Matrix Anal. Appl.*, 44(1):382–407, 2023.
- [20] Z. Jia and Y. Yang. A joint bidiagonalization based iterative algorithm for large scale general-form Tikhonov regularization. *App. Numer. Math.*, 157:159–177, 2020.
- [21] P. Jolivet, J. E. Roman, and S. Zampini. KSPHPDDM and PCHPDDM: Extending PETSc with advanced Krylov methods and robust multilevel overlapping Schwarz preconditioners. *Comput. Math. Appl.*, 84:277–295, 2021.
- [22] M. E. Kilmer, P. C. Hansen, and M. I. Español. A projection-based approach to general-form Tikhonov regularization. *SIAM J. Sci. Comput.*, 29(1):315–330, 2007.
- [23] C. C. Paige and M. A. Saunders. Towards a generalized singular value decomposition. *SIAM J. Numer. Anal.*, 18(3):398–405, 1981.
- [24] C. C. Paige and M. A. Saunders. LSQR: an algorithm for sparse linear equations and sparse least squares. *ACM Trans. Math. Software*, 8(1):43–71, 1982.
- [25] B. N. Parlett. *The Symmetric Eigenvalue Problem*. Prentice-Hall, Englewood Cliffs, NJ, 1980. Reissued with revisions by SIAM, Philadelphia, 1998.
- [26] J. E. Roman, C. Campos, L. Dalcin, E. Romero, and A. Tomas. SLEPc users manual. Technical Report DSIC-II/24/02–Revision 3.18, D. Sistemes Informàtics i Computació, Universitat Politècnica de València, 2022.
- [27] Horst D. Simon and Hongyuan Zha. Low-rank matrix approximation using the Lanczos bidiagonalization process with applications. *SIAM J. Sci. Comput.*, 21(6):2257–2274, 2000.
- [28] C. F. van Loan. Generalizing the singular value decomposition. *SIAM J. Numer. Anal.*, 13(1):76–83, 1976.
- [29] Kesheng Wu and Horst Simon. Thick-restart Lanczos method for large symmetric eigenvalue problems. *SIAM J. Matrix Anal. Appl.*, 22(2):602–616, 2000.
- [30] H. Zha. Computing the generalized singular values/vectors of large sparse or structured matrix pairs. *Numer. Math.*, 72(3):391–417, 1996.